3rd International Congress on Durability of Concrete
22 - 25 October 2017, Adelaide, Australia, p. 9.
Paper 19948

Mechanical and durability properties of a concrete using magnesium silicate hydrate binder system

Hung Tran[1], Allan Scott[2], Rajesh Dhakal[3], and Nan Yang[4]
[1]PhD Candidate in Civil Engineering, University of Canterbury
[2]PhD, Senior Lecturer of Concrete Materials, University of Canterbury
[3]Professor of Civil Engineering, University of Canterbury
[4]PhD Candidate in Civil Engineering, University of Canterbury

Abstract: Magnesium silicate hydrate (M-S-H) binder systems containing reactive magnesium oxide and amorphous silica have been increasingly studied since its cementitious properties were first reported in 2006. This paper presents an experimental study of mechanical and durability properties of a concrete using an M-S-H binder system containing 60% MgO and 40% SiO_2. The compressive strength of M-S-H samples at 28 days was approximately 40 MPa. The MSH concrete developed its strength more slowly than the PC mix over the 28 days curing period. Other mechanical properties (split tensile strength and modulus of elasticity) of M-S-H concrete were also lower than the comparable PC samples. Concrete samples using M-S-H binders showed moderate to good durability indexes (porosity, oxygen permeability, resistivity) for durable concretes. The PC concrete samples were generally less porous/permeable and accordingly performed better than M-S-H concrete in terms of durability.

Keywords: Magnesium silicate hydrate, reactive magnesium oxide, silica fume, strength, durability.

1. Introduction

Research on alternative binder systems for Portland cement has increased considerably due to the urgent need to reduce CO_2 emissions from the cement production process. The synthesis M-S-H binder systems are known to have a lower impact on the environment compared to Portland cement (PC), in part due to calcination at low temperatures (700-1000^{o}C). There are also potential uses of M-S-H binders for the immobilization of nuclear wastes (1).

The mechanical properties of M-S-H pastes and mortars have been reported in the literature with a wide range of strength values. Wei et al. (2) was among the first authors reporting cementitious property of M-S-H mortars of over 50 MPa. Zhang et al. (3) developed M-S-H binder systems for immobilization of nuclear wastes obtaining strength of over 60 MPa. Marmol et al. (4) studied M-S-H and Portland cement pastes in which M-S-H samples achieved superior strength compared to PC samples at a similar water to cement ratio. Tran and Scott (5) optimized ternary mixtures of MgO-SiO_2-quartz filler resulting in strengths exceeding 85 MPa. On the other hand, Jin and Al-Tabbaa (6) and Walling et al. (7) reported fairly low strengths of M-S-H binder systems due to the very high water content for workability. The strength of M-S-H binders however strongly depends on the material sources (8).

The reaction mechanism of MgO-SiO_2 mixtures has been studied widely in which MgO/SiO_2 ratio has large effect to the hydration products. Zhang (3) reported that all of the brucite reacted with silica fume (SF) to form M-S-H gel in mixtures containing 60% SF and 40% MgO. Wei (2) showed that at higher MgO/SiO_2 ratios, residual brucite and M-S-H phases co-existed in the resulting pastes (2). The Mg/Si molar ratio was found to be lower than Ca/Si in Portland cement (9) and varied in a range of 0.7-1.5 (10).

This paper studied the possibilities of producing a strong and durable M-S-H concrete. The properties of one of the first concretes using M-S-H binder systems composed of common materials available in the construction industry were reported. Binders containing 60% MgO – 40% SiO_2 was selected to compare with control Portland cement samples. Basic mechanical and durability properties of M-S-H concrete were tested to examine potential uses of M-S-H binders for construction materials in large scale.

2. Experimental programme

2.1 Materials

The reactive magnesia calcined from magnesite at temperature of below 700°C was supplied by Calix Ltd. (Australia). Silica fume, a highly reactive silica source, was provided by Sika NZ in condensed form with the following properties: bulk density of 660kg/m^3, 95% of total SiO_2, and surface area of 27.3 m^2/g. The aggregates including local river sand (max particle size of 4.75 mm) and stone (max aggregate size of 16 mm) were obtained from local regions. The particle size distribution of MgO and silica fume was determined by LA-950 Laser particle size analyzer. Conglomerates of condensed silica fume have large particle size compared to original silica fume particles (11). Sieving method was used for fine and coarse aggregates (Figure 1).

Due to the high volume of silica fume, the use of a superplasticizer was crucial to ensure workability. Based on a previous study (5), the Viscocrete-5-555 superplasticizer (VC), which resulted in higher water reduction effect for workability, was selected.

Control samples were prepared using Ultracem cement which is a general purpose Portland cement (Type GP) provided by Holcim New Zealand.

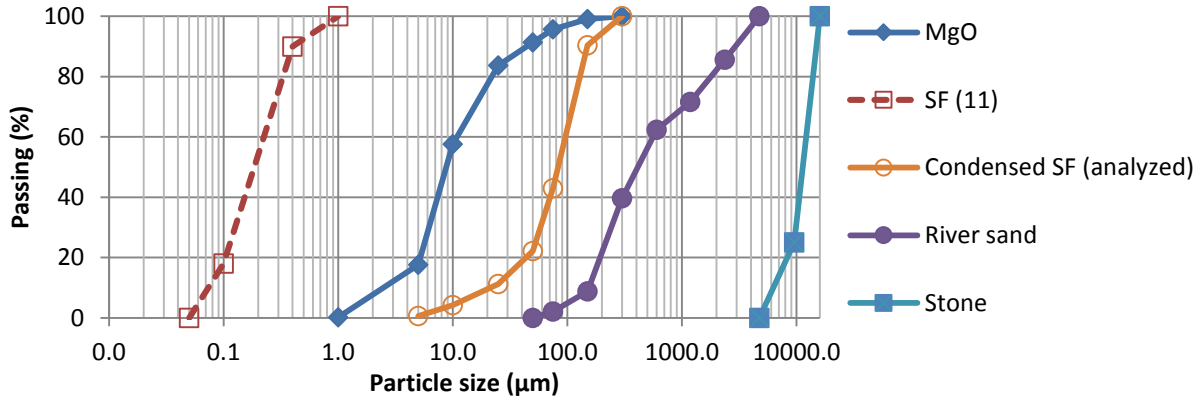

Figure 1. Particle size distribution of materials.

2.2. Mix proportions

Mix proportions and sample labels are presented in Table 1. An MgO/SiO_2 ratio of 60/40 weight percent (wt. %) was selected based on its optimal strength performance compared to other MgO/SiO_2 ratios (5). The sand and stone content for MSH and control PC concretes were based on typical PC concrete mixes.

Table 1. Mix proportions (by mass)

Mix label	PC	MgO	Silica fume	Sand/c	Stone/c	w/c	SP (% binder, liquid)
MSH	-	0.6	0.4	1.25	2.0	0.40	3% VC
PC	1.0	-	-	1.25	2.0	0.40	-

2.3. Samples preparation and testing procedure

A pan mixer was used to mix MSH concrete while PC concrete was mixed by a drum mixer. Samples were cast in 100 mm diameter × 200 mm height cylindrical moulds and demolded after 24 h before curing in water at 20°C until tested at 7 and 28 days age. Mechanical property and durability tests include:

2.3.1. Mechanical property tests

Compressive strength was determined according to ASTM C 39. Cylindrical samples were cast in 100 mm diameter × 200 mm height molds. Three samples of each mixture were tested to calculate the average value as the compressive strength result.

Split tensile strength test was performed instead of direct tensile test. The testing procedure is in accordance with the ASTM standard C 496 using cylindrical sample size of 100 mm × 200 mm.

The static modulus of elasticity (MOE) of the MSH concrete and PC specimens was tested as per ASTM C 469 on 100 mm diameter × 200 mm height cylindrical specimens.

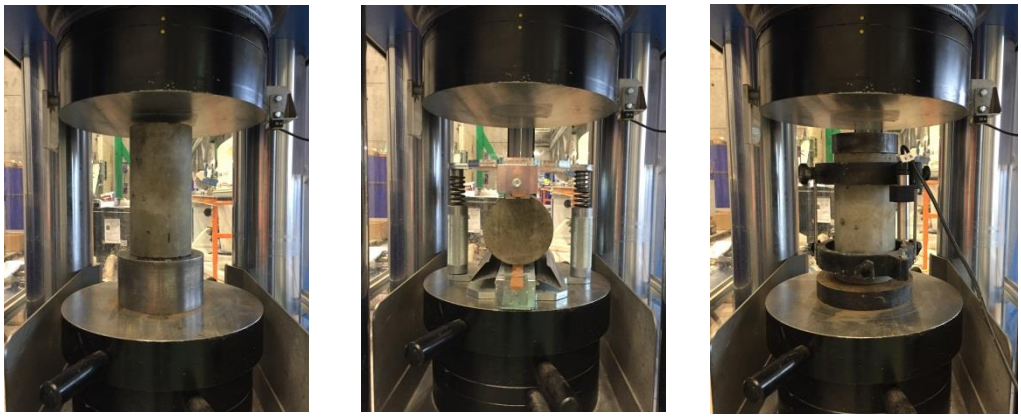

(a) (b) (c)

Figure 2. Mechanical testing setup
(a): Compressive strength, (b): Split tensile strength, (c): Modulus of elasticity.

2.3.2. Durability tests

Porosity presented by percent voids in hardened cementitious materials was determined as per ASTM C 642 with some modifications. Four testing cylinders were cut from 100 × 200 mm concrete cylindrical samples to have thickness of 30 ± 3 mm. Instead of submerging specimens in boiling water, a vacuum chamber was applied to remove the entrapped air before immersing in water at ambient temperatures (21^{o}C) to determine surface-dried and apparent mass. Porosity is calculated in formula of volume of permeable pore space voids:

$$P(\%) = (C - A)/(C - D) \times 100$$

where:

A = oven-dried mass in air, g

C = surface-dried mass in air after vacuumed and immersed in water, g

D = apparent mass in water after vacuumed and immerged in water, g

2.3.5. Oxygen Permeability Index

The Oxygen Permeability Test (OPT) was performed to determine Oxygen Permeability Index (OPI), which is related to the durability of the testing concrete. A falling head permeameter was used to apply pressure to a concrete sample in which the pressure is allowed to decay as permeation proceeds. The faster reduction rate of pressure indicates higher gas (oxygen) permeability and possibly a reduction in the durability of the concrete (12).

Four cylinders of 30± 2 mm thick were cut from 100 × 200 mm concrete cylinders. Each sample was inserted in a compressible rubber collar, placed in the upper cell and then compressed so that no gaps should be visible between the sides of the test specimen and the collar. An initial pressure was set at 100 kPa and the test was terminated as the pressure reduced to 50 kPa or after 6 hours.

Calculation of the OPI required determining pressure decay curve which was plotted in the form of logarithm of ratio of pressure heads over the time, based on the D'arcy coefficient of permeability:

$$k = \frac{\varpi V g d}{R A \theta} \ln \frac{P_0}{P}$$

where:

k = coefficient of permeability of test specimen (m/s)

ω = molecular mass of oxygen = 32 g/mol

V = volume of oxygen under pressure in permeameter (m^3)

g = acceleration due to gravity (9.81 m/s^2)

R = universal gas constant = (8.313 Nm/K mol)

d = average specimen thickness (m) to the nearest 0.02 mm

A is the cross sectional area of the specimen (m^2)

θ= absolute temperature (K)

The OPI was taken as the negative log of the average of the coefficients of permeability of the tested specimens, which was determined by the following equation:

$$OPI = -\log 10\left[\tfrac{1}{4}(k_1 + k_2 + k_3 + k_4)\right]$$

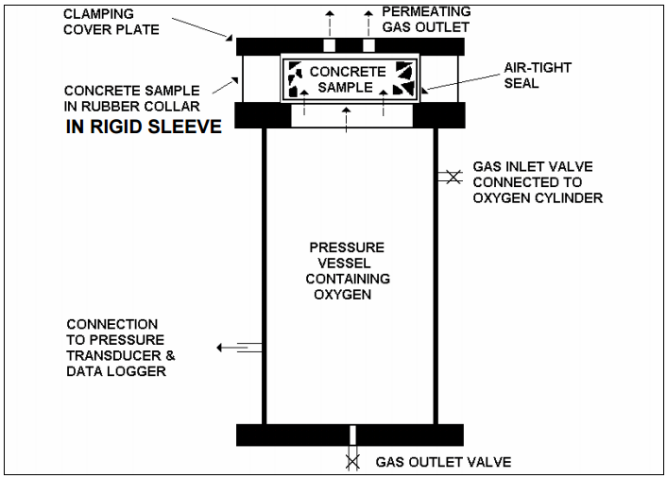

Figure 3. Permeability cell arrangement (12).

2.3.6. Resistivity

Resistivity test is a fast measurement technique which provides comparable results to the RCPT (13). The resistivity test reused the samples as described in OPI tests. After re-drying to a constant mass the samples were soaked in 3.5% NaCl solution in 22 h until saturated, the resistivity was measured from the applied voltage and corresponding current across the sample:

$$R = \left(V/I\right) \times \left(A/d\right) \text{ (kOhm.cm)}$$

V = applied voltage (mV)

I = current at 1 min (μA)

A = cross sectional area of the specimen (cm^2)

d = average specimen thickness (cm)

3. Result and discussions

3.1. Mechanical properties

Compressive strength of MSH and PC concrete is shown in Figure 4. It is apparent that the MSH concrete has a lower compressive strength at all ages compared to PC concrete. At 7 days age, the MSH concrete obtained strength of over 20 MPa while PC concrete obtained over 50 MPa. At the 28 days age, the MSH concrete increased strength by 75% to 40 MPa while this increase of PC concrete was only 21% to 62 MPa. The compressive strength of MSH concrete is possibly sufficient for a wide range of structural applications.

The strength development rate of MSH sample is slightly slower than PC concrete in which MSH samples at 7 days age obtained 60% 28-day strength. On the other hand, the PC samples at 7 days achieved over 80% of 28-day strength. This slow strength development might be a result of the slow hydration process of MSH binder systems in which the strength gain is mainly attributed to the pozzolanic reaction of brucite and silica to form magnesium silicate hydrate binding gels.

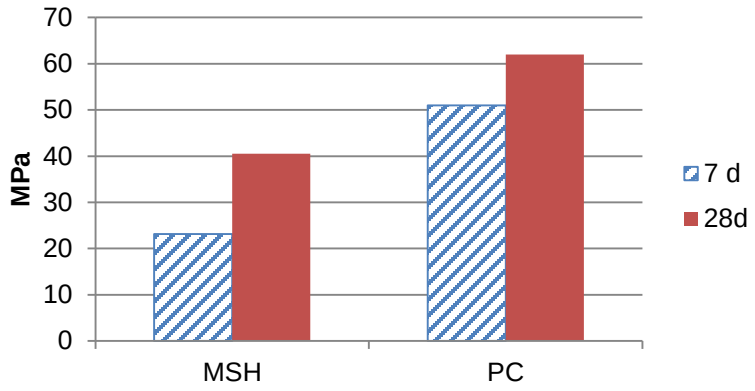

Figure 4. Compressive strength of MSH and PC concrete

Figure 5 presents split tensile strength of MSH and PC concrete. The split tensile strength of MSH concrete is dramatically lower than PC concrete. MSH concrete appears more brittle than PC concrete.

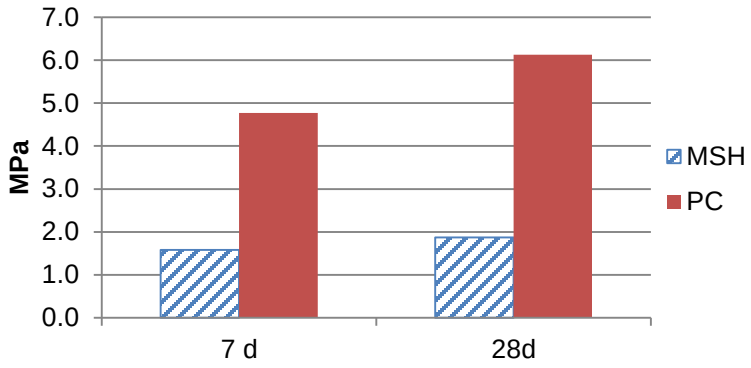

Figure 5. Split tensile strength of MSH and PC concrete

Figure 6 and figure 7 show stress-strain relations in which Modulus of elasticity (MOE) of MSH and PC samples were determined. As loading up to 40% of the compressive strength, the linear stress-strain behavior was observed up to a very low loading range of about 10% of the compressive strength followed by the nonlinear stress-strain behavior. These nonlinear relations were linearly idealized for the ease of

comparison with MOEs of PC. The MSH concretes showed linearly idealized MOEs of 7.885 GPa and 10.888 GPa at 7 and 28 days age (respectively). These values are fairly low compared to the MOEs of PC control samples, which were 33.481 GPa and 38.635 GPa at 7 and 28 days age (respectively). The low MOEs of MSH concrete might limit its application for some structures restraining deflection/deformation. Further investigation into the stress strain response of MSH concrete is necessary for this rather unusual material.

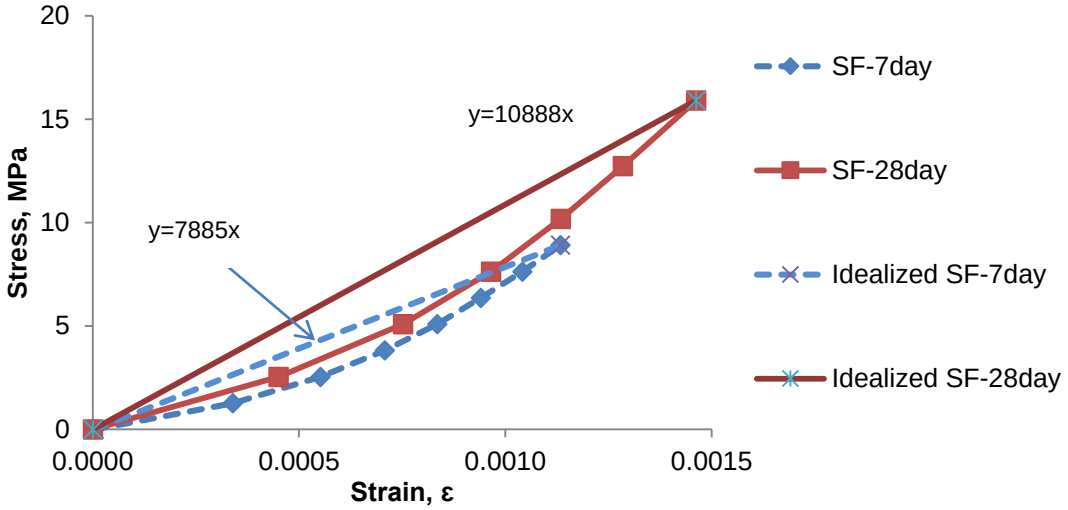

Figure 6. MOE of MSH concrete

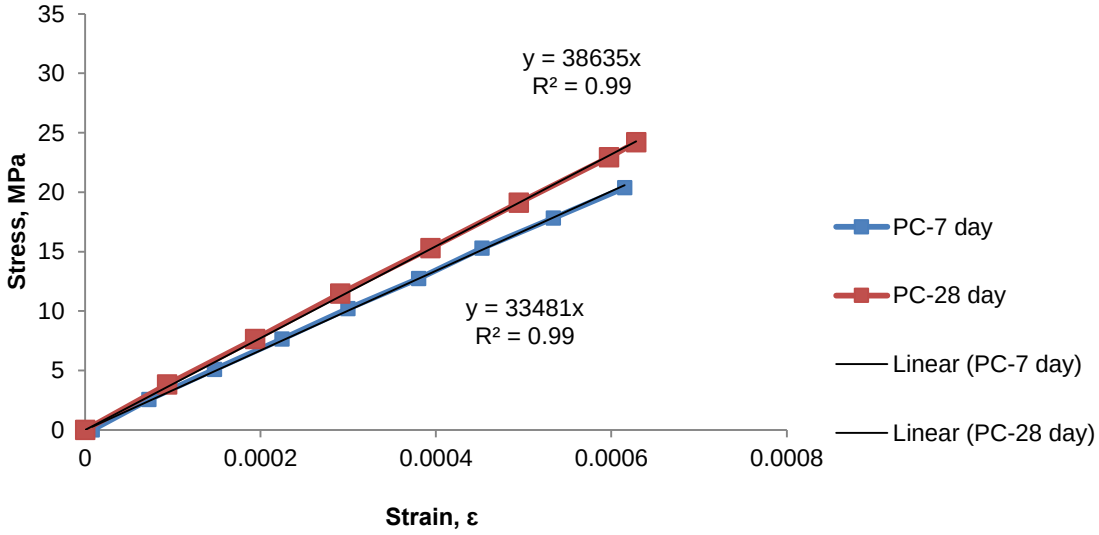

Figure 7. MOE of PC concrete

3.2. Durability

Figure 8 shows porosity of MSH and PC concretes. Substitution of PC by M-S-H binder increased the void ratio of the concrete mixture, however, still resulted in low porosity concrete for durability. The difference in voids between 7 and 28 days age is negligible.

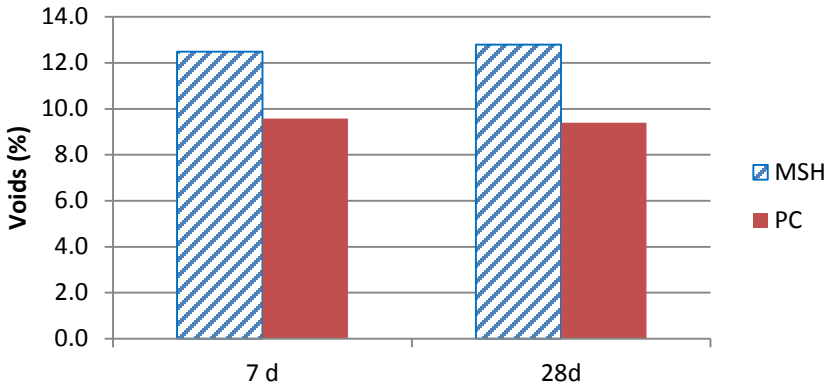

Figure 8. Porosity of PC concrete

Figure 9 presents permeability coefficients of MSH and PC concrete at 7 and 28 days age. Interpretation of the permeability coefficients and OPI for the durability was suggested by Alexander et al. (12) (Table 2).

Table 2. Durability classification using index values (adapted from Alexander et al. (12))

Durability class	OPI (log scale)	k (10^{-10})
Excellent	>10	1
Good	9.5-10	1-3.16
Poor	9.0-9.5	3.16-10
Very poor	<9.0	>10

A low OPI (or high permeability coefficient) suggests high or interconnected porosity and therefore poor durability. Permeability coefficients of MSH samples increased in the curing duration from 7 to 28 days while those of PC reduced marginally. All samples have permeability coefficients lower than 3.16 which indicate the good and excellent durability although the MSH binder resulted in higher oxygen permeability than PC.

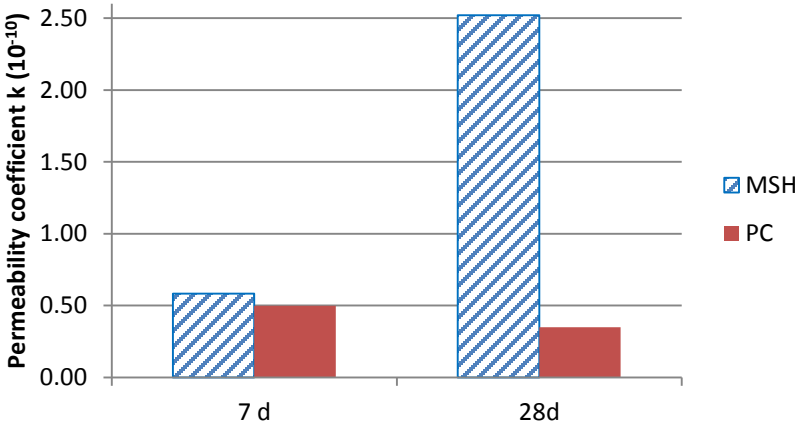

Figure 9. Permeability coefficients of MSH and PC concrete

The resistivity (also called bulk resistivity) was used to evaluate the Chloride Ion Penetration of the MSH and control PC concrete samples. High resistivity resulted from low permeability and therefore indicates good durability concrete. There have been a number of studies on the correlation of the Rapid Chloride Penetration (RCP), Surface Resistivity and Resistivity tests. Gudimettla and Crawford (13) and Spragg

et.al. (14) suggested a 1.9 times higher of SR compared to resistivity as measured in this study. Table 3 shows the relation of RCP Test and Resistivity using the conversion factor of 1.9.

Table 3. Chloride Ion Penetration and resistivity classification

(Adapted from Gudimettla and Crawford (13) and AASHTO (15))

Chloride Ion Penetration	RCP Test Charges Passed (Coulombs)	Surface Resistivity Test 4"x8" Cylinder (KOhm-cm)	Bulk Resistivity Test 4"x8" Cylinder (KOhm-cm)
High	> 4,000	< 12	<6.3
Moderate	2000-4000	12 – 21	6.3-11
Low	1000-2000	21 – 37	11-19.5
Very Low	100-1000	37 – 254	19.5-134
Negligible	<100	> 254	>134

The resistivity of MSH and PC samples at 7 and 28 days is presented in Figure 10. MSH concrete showed a slightly decreased resistivity compared to PC samples. The resistivity of both MSH and PC samples increased over the curing period up to 28 days. Resistivity of MSH concrete ranged of 6.8 to 10.3 to indicate a moderate Chloride ion penetration level as referred to Table 3. The PC control concrete samples at 28 days age had higher resistivity of below 12 kOhm.cm, suggests a low Chloride ion penetration.

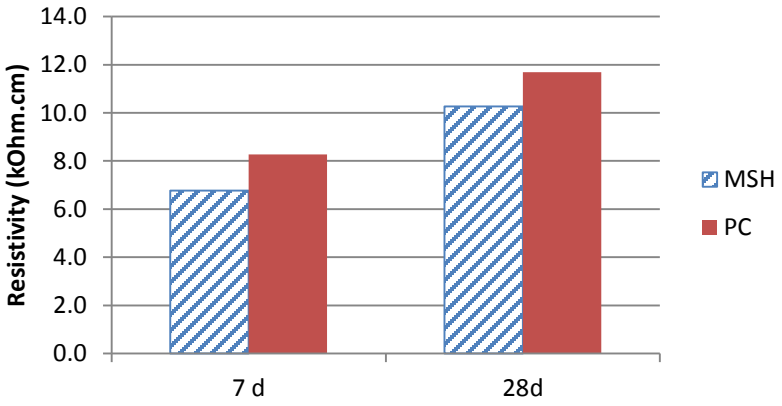

Figure 10. Resistivity of MSH and PC concrete.

4. Conclusion

A binder composition of reactive magnesium oxide and silica fume (60%MgO – 40% SiO_2) enables the production of concrete with 40MPa at 28 days age. The strength development of MSH concrete is somewhat slower than the control PC concrete.

The used M-S-H binder system results in lower tensile strength and Modulus of elasticity compared to PC concrete. Concrete using M-S-H binder also shows a non-linear stress-strain relationship in the loading range up to 40% of compressive strength.

The concrete using PC performed slightly better than M-S-H concrete in durability tests. However, the testing M-S-H concrete had durability indexes of moderate to good class which indicates potential uses even in aggressive environment.

This study only tests an M-S-H binder system containing 60% MgO and 40% silica fume. As the MgO/SiO_2 ratio and material sources significantly influence the properties of the MSH binder, these effects needs to be investigated further for the M-S-H binder concretes.

5. References

1. Zhang, T., Vandeperre, L.J., and Cheeseman, C.R., “Magnesium-silicate-hydrate cements for encapsulating problematic aluminium containing wastes”, Journal of Sustainable Cement-Based Materials, 1 (1-2), 2012, pp 34-45.
2. Wei J.X, Chen Y.M, Li Y.X., “The Reaction Mechanism between MgO and Microsilica at Room Temperature”, Journal of Wuhan University of Technology - Mater. Sci. Ed. 21(2), 2006, pp 88-91.
3. Zhang, T., Vandeperre L.J., Cheeseman C.R., “Formation of magnesium silicate hydrate (M-S-H) cement pastes using sodium hexametaphosphate”, Cement and Concrete Research, 65, 2014, pp 8–14.
4. Mármol, G., Savastano, H., Tashima, M. M., & Provis, J. L., “Optimization of the MgO-SiO_2 binding system for fiber-cement production with cellulosic reinforcing elements”, Materials & Design, 105, 2016, pp 251-261.
5. Tran, H. M., & Scott, A., “Strength and workability of magnesium silicate hydrate binder systems”, Construction and Building Materials, 131, 2017, pp 526-535.
6. Jin F., Al-Tabbaa A., “Strength and hydration products of reactive MgO–silica pastes”, Cem. Concr. Compos. 52, 2014, pp 27–33.
7. Walling S. A., Kinoshita H., Bernal S. A., Colliera N. C., and Provis J. L. ”Structure and properties of binder gels formed in the system $Mg(OH)2–SiO_2–H_2O$ for immobilisation of Magnox sludge”, The Royal Society of Chemistry, Dalton Trans., 44, 2015, pp 8126–8137.
8. Jin, F., Gu, K., Abdollahzadeh, A., & Al-Tabbaa, A., “Effects of different reactive MgOs on the hydration of MgO-activated GGBS paste”, Journal of Materials in Civil Engineering, 27(7), 2013.
9. Lothenbach B., Nied D., L’Hopital E., Achiedo G., Dauzeres A., “Magnesium and calcium silicate hydrates”, Cem. Concr. Res. 77, 2015, pp 60–68.
10. Nied D., Enemark-Rasmussen K., L'Hopital E., Skibsted J., & Lothenbach B., “Properties of magnesium silicate hydrates (M-S-H)”, Cement and Concrete Research, 79, 2016, pp 323-332.
11. Malhotra, V.M., Ramachandra, V.S., Feldman, R.F., Aitcin, P.C., “Condensed silica fume in concrete”, No. 5657JD, 1987, CRC Press.
12. Alexander, M. G., Mackechnie J. R., and Ballim Y., "Guide to the use of durability indexes for achieving durability in concrete structures", Research monograph 2, 1999.
13. Gudimettla, J.M., Crawford, G.L., “Field Experience in using Resistivity Tests for Concrete”, in Transportation Research Board 94th Annual Meeting (No. 15-3357), 2015.
14. Spragg R., Bu Y., Snyder K., Bentz D., and Weiss J., “Electrical Testing of Cement Based Materials: Role of Testing Techniques, Sample Conditioning, and Accelerated Curing”, Publication FHWA/IN/JTRP-2013/28. Joint Transportation Research Program, Indian Department of Transportation and Purdue University, West Lafayette, Indiana, 2013.
15. AASHTO TP-95. Surface Resistivity Indication of Concrete’s Ability to Resist Chloride Ion Penetration, 2011, Washington, D.C.